

Internal Vortex Structure of a Trapped Spinor Bose-Einstein Condensate

S.-K. Yip

Physics Division, National Center for Theoretical Sciences, P. O. Box 2-131, Hsinchu, Taiwan 300, R. O. C.
(May 17, 2019)

The internal vortex structure of a trapped spin-1 Bose-Einstein condensate is investigated. It is shown that it has a variety of configurations depending on, in particular, the ratio of the relevant scattering lengths and the total magnetization.

PACS number: 03.75.Fi

Recently the MIT group has succeeded in obtaining Bose Einstein Condensation (BEC) of ^{23}Na atoms in an optical trap. [1,2] A novel aspect of this system is that ^{23}Na atoms possess a hyperfine spin, with $f = 1$ in the lower multiplet. All three possible projections of the hyperfine spin can be optically trapped simultaneously. Thus generally the condensate have to be described by a spin-1 order parameter consisting of the spinor (Ψ_u, Ψ_0, Ψ_d) where $\Psi_{u,0,d}$ are the macroscopic wavefunctions with the hyperfine projection $s = 1, 0, -1$ respectively. The ground state of the condensate is determined by the spin-dependence of the interaction between the bosons. [3,4] In the dilute limit they can be characterized by the (s-wave) scattering lengths a_0 and a_2 in the total (hyperfine-)spin 0 and 2 channels respectively. The polar state, where the order parameter is proportional to the spinor $(0, 1, 0)$, is favored if $a_2 > a_0$, but the axial state, where the spinor is $(1, 0, 0)$, if the inequality is otherwise. ^{23}Na belongs to the former case. However, ^{87}Rb is predicted to belong to the latter case. [3]

A particular interesting feature of these systems is that, due to the weak spin dependence of the interatomic interaction, $a_0 \approx a_2$. For example for ^{23}Na $a_0 \approx 46a_B$ and $a_2 \approx 52a_B$, where a_B is the Bohr radius. Thus the difference $a_2 - a_0 \approx 6a_B$ is only a small fraction of a_0 or a_2 . As a result, the condensate only needs to pay very little extra energy to get into the “wrong” state. If there is a competing energy, such as that due to the presence of a gradient, it may be energetically favorable for the condensate to deviate locally from the polar state. An analogous remark is also applicable to ^{87}Rb , where $a_0 \approx 110a_B$ and $a_2 \approx 107a_B$. [5]

In this paper I shall illustrate this by considering vortices of this spin-1 Bose condensate. Vortices with a scalar order parameter in BEC has been discussed in many papers (e.g [6,7]). In a cylindrically symmetric trap, there is no stable state for angular momentum $L < N\hbar$ where N is the number of particles. A singly quantized vortex has $L = N\hbar$, with the position where the order parameter is singular located at the center of the trap. Here I shall show that vortices in a spinor condensate is even more interesting in that they exhibit a

very rich internal structure. In general locally the order parameter is in neither the polar nor the axial state. They may have broken cylindrical symmetry with vortices of individual species appearing at positions other than the trap center. The minimum angular momentum required for the formation of the vortex is also less than N . Moreover transitions between different internal vortex structures are possible. Vortices were also discussed in Ref [3] and [4], but they did not consider structures which arise from deviations of the order parameter from the original polar or axial phases.

Since the order parameter has more than one component, it is convenient to distinguish between vortices of individual order parameter component Ψ_s and the composite structure. I shall refer the latter as the composite vortex (CV).

The order parameter, in particular that of the CV, is found by minimization of the energy (restricting ourselves to $T = 0$) under appropriate constraints. The energy density \mathcal{E} consists of the kinetic and potential contributions $\sum_s \frac{|\nabla\Psi_s|^2}{2M_a} + V|\Psi_s|^2$, where M_a is the atomic mass, V is the trap potential and the sum is over all spin components, and the interaction part which can be written as $\mathcal{E}_{\text{int}} = \frac{1}{2}(c_0 + c_2)n^2 - \frac{1}{2}c_2|2\Psi_u\Psi_d - \Psi_0|^2$ where $n = \sum_s |\Psi_s|^2$ is the local density. Here $c_0 \equiv \frac{g_0 + 2g_2}{3}$ and $c_2 \equiv \frac{g_2 - g_0}{3}$ where $g_{0,2}$ are in turn related to the scattering lengths in the total spin 0 and 2 channels via $g_{0,2} = \frac{4\pi\hbar^2 a_{0,2}}{M_a}$. [3] The total particle number N , angular momentum L and magnetization M should be considered as conserved if no exchange of the corresponding quantity is allowed between the atoms inside the trap and their environment (within the relevant experimental time scale). In this case we have to minimize the total energy for given N , L and M . As usual it is convenient to introduce and minimize the free energy $G \equiv E - \mu N - \Omega L - HM$ where μ , Ω and H are Lagrange multipliers. μ , Ω , H correspond to the chemical potential, angular velocity and magnetic field. Ω is given by the angular velocity of the rotating trap if angular momentum can be exchanged between the trapped atoms and their environment.

It is useful to note that the energy is invariant under relative rotation between the real and spin space. Accordingly below the spin quantization axis will be chosen for the most convenient presentation (and always along the total magnetization if it is finite). In particular the configurations presented below do not rely on any special relative orientation between the net magnetization and the rotational axis (which is always chosen as z). Since the rotational properties of magnetization is intuitively

much simpler than that of a spin-1 wavefunction, I shall also discuss the local magnetization density \vec{m} . The projection of \vec{m} along a general direction is measurable in BEC experiments since it is given by the difference in the number density between the u and d species when one uses that direction as the quantization axis.

Setting the variation of the free energy with respect to Ψ_s^* to zero, one obtains the familiar Gross-Pitaevskii (GP) equations (generalized due to the presence of multiple spin species [3,4]). If $c_2 > 0$ such as in the case of ^{23}Na , in the absence of a net magnetization the order parameter can be *chosen* so that only Ψ_0 is finite and obeys the GP equation in the usual form: $0 = (-\frac{\hbar^2}{2M_a}\nabla^2 + V - \mu)\Psi_0 + c_0|\Psi_0|^2\Psi_0$. The order parameter profile for Ψ_0 would then be completely analogous to that of a scalar order parameter with the interaction parameter given by c_0 (note then Ψ_0 is independent of c_2). In particular in the absence of any circulation and if one ignores the gradient term, (the Thomas Fermi (TF) approximation [8]) $|\Psi_0|^2 = \frac{\mu-V}{c_0}\theta(\mu-V)$. The structure of a singly quantized vortex would also be exactly analogous to that of a scalar order parameter investigated by, *e.g.*, Dodd et al [6]. For the discussions below it is also convenient to re-consider the same CV with quantization axis rotated by $\pi/2$ about a horizontal axis. In this basis the above CV becomes two coinciding vortices of the u and d components with $|\Psi_u| = |\Psi_d|$ and with the vortices at the trap center. We shall see below that in general the CV is very different from the ones just discussed.

Typically in the experiments the cloud is trapped by a potential harmonic in all three spatial directions. For numerical simplicity I shall instead consider a cloud subject to a harmonic potential only in the $x-y$ plane but of uniform density within thickness d along the rotational z axis. It is reasonable to assume that the results below will be qualitatively applicable to a pancake shaped cloud trapped by a three dimensional, axially symmetric harmonic potential if the radii of the clouds perpendicular to the rotational axis are comparable. Rather than varying μ and Ω to obtain a fixed total number of particles and angular momentum, I shall simply present the types of CV for fixed μ 's and Ω 's. However, I shall continue to use the total magnetization (rather than H) as an independent variable [2]. I shall eliminate μ in favor of $R \equiv (2\mu/M_a\omega_o^2)^{1/2}$, where ω_o is the (angular) trap frequency. In the absence of vortices and under the TF approximation, the radius of the cloud and the total number of particles are independent of the value of c_2 and given by R and $N_o = \frac{d}{16a}(\frac{R}{\lambda_o})^4$ respectively, where λ_o is the size of the harmonic oscillator ground state wavefunction ($\lambda_o = (\hbar/M_a\omega_o)^{1/2}$). Here $a \equiv \frac{(a_0+2a_2)}{3}$ is an effective scattering length for the interaction parameter c_0 . All the CV presented below has $N \approx N_o$. [9]

I shall introduce the parameter $\epsilon \equiv (\lambda_o/R)^2$ which measures the deviation from the TF ($\epsilon \rightarrow 0$) limit. ϵ depends only weakly on N for given trap parameters. I

shall express Ψ_s in units of $\sqrt{\mu/c_o}$ (correspondingly the number density n and the magnetization density \vec{m} in μ/c_o) distances in units of R , and total particle number and magnetization m_{tot} in units of N_o . With this, all physical results depend only on the dimensionless parameters ϵ , $\tilde{\Omega} \equiv \Omega/\omega_o$, $\tilde{c}_2 \equiv c_2/c_o$ and m_{tot} . Anticipating future experiments on other atoms I will not fix \tilde{c}_2 to that of ^{23}Na (though confining myself to $\tilde{c}_2 > 0$). As a concrete example I shall consider mainly $\epsilon = 0.1$, $\tilde{\Omega} = 0.45$, [10] with the corresponding phase diagram shown in Fig. 1. I shall comment on other values of the parameters as I proceed.

We begin by considering $m_{\text{tot}} = 0$. I shall present the CV in two ways, each related to some of the CV structures discussed for $m_{\text{tot}} \neq 0$ below. The structure of the CV with quantization axis chosen so that it resembles most closely a vortex of Ψ_0 alone is as shown in Fig. 2. However, instead of an empty core, it is energetically favorable for some of the 0 particles to convert to u and d species and appear near the center of the trap. For the present parameters, $|\Psi_u| = |\Psi_d|$ and each has two vortices. In Fig 2 the order parameter along the line (chosen as the x axis) going through these vortices was shown. Note that the CV has broken cylindrical symmetry.

Another useful way of presenting the above CV is to use quantization axis rotated by $\pi/2$ about a horizontal axis with respect to those above. In this basis only Ψ_u and Ψ_d are finite, and both have a unit circulation with the Ψ_u and Ψ_d vortices displaced by equal but opposite distance from the trap center (Fig 3). It follows that the local magnetization density is finite and points along the (present) \hat{z} -axis, being negative for $x < 0$ and positive for $x > 0$. Notice that at the vortex for say the d -component, since $|\Psi_d| = 0$ and $|\Psi_u| \neq 0$, locally the condensate is actually in the axial but not polar state (even though m_{tot} and H are zero)

With the use of this quantization axis we can also understand easily the reason for the present CV structure. Due to the presence of the trap potential a vortex has maximum kinetic energy if it is located at the center of the trap. It is energetically favorable to move the u and d vortices away from the trap center. [6,7] For the system to be at an energy minimum, the u and d vortices move opposite to each other, creating regions where $|\Psi_u| \neq |\Psi_d|$, eventually balanced by the desire of the condensate to remain in the polar state. In this picture it is obvious that $L/N < 1$. As Ω increases, the $\Psi_{u,d}$ vortices move closer to the center of the trap and L/N increases. [*e.g.*, for $\tilde{c}_2 = 0.2$, $L/N = 0.87(0.92)$ at $\tilde{\Omega} = 0.45(0.5)$]. The separation between the vortices, and the region where the local magnetization is non-zero, increases with decreasing \tilde{c}_2 [correspondingly L/N decreases: *e.g.*, at $\tilde{\Omega} = 0.45$, $L/N = 0.84(0.80)$ for $\tilde{c}_2 = 0.1(0.05)$]

Now we are ready to consider the structure of the CV with finite total magnetization. I shall describe each region of the phase diagram Fig. 1 in turn.

I: In this region the favorable configuration is similar

to that of Fig 3 except for an increase (decrease) in the amplitude of Ψ_u and Ψ_d (not shown). The local and total magnetization of this CV are always collinear. One can understand this configuration by considering the energy under the magnetic field H . The CV has an order parameter and hence a magnetic susceptibility which is anisotropic. For a given magnitude of the magnetization, the energy is minimum if the direction of \vec{m}_{tot} is along that of largest susceptibility. The quantization axes used in Fig 2 and 3 above correspond to the principal directions of the susceptibility tensor. It is intuitively reasonable that the CV has larger susceptibility along the quantization axis of Fig 3 (*c.f.* [4]).

II: For larger m_{tot} the vortex of the minority species d disappears. The CV is replaced by a vortex of the u species with a d core. (Fig. 4.) This can be understood by recognizing that the effective chemical potential for the d species is given by $\mu - H$. Increasing m_{tot} requires increasing H , hence decreasing $\mu - H$. Eventually the effective chemical potential is too low to overcome the necessary kinetic energy required for forming a circulating d component. This picture is supported by the fact that the critical m_{tot} needed for the I \rightarrow II transition increases with Ω . The $-\Omega L$ term in the free energy favors an order parameter with finite circulation, thus at higher angular velocity a larger H and hence m_{tot} is required for the transition. [*e.g.*, at $\tilde{c}_2 = 0.2$, the critical $m_{\text{tot}} \approx 0.2$ for $\tilde{\Omega} = 0.45$ here (Fig 1) whereas $m_{\text{tot}} \approx 0.4$ for $\tilde{\Omega} = 0.5$]

III: This occurs at still larger m_{tot} and only for small c_2 . In this region the CV has a u vortex with a core filled by the 0 species (Fig 5) The minimum magnitude of m_{tot} needed for this new CV increases with \tilde{c}_2 . These features can be understood by considering again the effective chemical potential for the 0 and d spins which are μ and $\mu - H$ respectively. The spin 0 species is more favored by H , but suffers a stronger repulsion (than the d species) from the majority u species due to the spin dependent interaction $c_2 (> 0)$. Only at sufficiently small c_2 and large m_{tot} does this CV become favorable.

In Fig. 6 we display the local magnetization density \vec{m} of this CV at points on the x axis, defined so that the phase difference between the u and 0 components vanishes for $x > 0$. Near the trap center \vec{m} points mainly along the horizontal, turning towards \hat{z} , the direction of net magnetization, only further away. The magnitude as well as the z -component of \vec{m} depends only on the radial distance from the center of the trap. The azimuthal angle of \vec{m} is the negative of that of the corresponding physical point in space. It is interesting to note that the presence of the CV may actually not be apparent if one examines only the particle number density n , in strong contrast to the case of a scalar condensate. [6].

IV: This is the most intriguing region. At very small \tilde{c}_2 (and not too small ϵ 's) the CV has spontaneous (spin) symmetry breaking in the sense that it has a net magnetization even when $H = 0$. The configuration evolves from that of Fig. 2 by the creation of an imbalance between

the number of spin-up (relative to spin-down) particles (see Fig 7) This configuration is stable so long as the total magnetization is close to that of the ‘spontaneous’ one, i.e. the topology of the CV remains the same except for a re-adjustment of the amplitudes of Ψ 's. The corresponding local magnetization density is as shown in Fig 8. The direction of \vec{m} thus rotates from $-\hat{x}$ through \hat{z} to \hat{x} as one moves along the physical x -axis. The existence of this spontaneous m_{tot} means more of the local order parameter is axial like, and thus this state is possible only for sufficiently small \tilde{c}_2 Upon further increase in m_{tot} , this configuration gives way to that of a u -vortex and a d core (Fig 4), which has a larger susceptibility, discussed earlier.

In conclusion I have shown that the internal vortex structure of a spin-1 Bose condensate in a harmonic trap is much richer than that of a condensate with a scalar order parameter. Observation of these objects would be interesting indeed.

I thank T.-L. Ho for his comments on the manuscript.

-
- [1] D. M. Stamper-Kurn *et al*, *Phys. Rev. Lett.* **80**, 2027, 2030 (1998)
 - [2] J. Stenger *et al*, *Nature*, **396**, 345 (1999)
 - [3] T. L. Ho, *Phys. Rev. Lett.* **81**, 742 (1998)
 - [4] T. Ohmi and K. Machida, *J. Phys. Soc. Jpn.*, **67**, 1822 (1998)
 - [5] These scattering lengths are as quoted in [3] and attributed to J. Burke, J. Bohn and C. Greene, unpublished.
 - [6] R. J. Dodd, K. Burnett, M. Edwards and C. W. Clark, *Phys. Rev. A* **56**, 587 (1997).
 - [7] D. S. Rokhsar, *Phys. Rev. Lett.* **79**, 2164 (1997).
 - [8] G. Baym and C. J. Pethick, *Phys. Rev. Lett* **76**, 6 (1996)
 - [9] For comparison for the cloud harmonically trapped in all three directions, the number of particles in the TF approximation is $N_o^{(3)} = \frac{R_z}{15a} (\frac{R}{\lambda_0})^4$ where $2R_z$ is the dimension of the cloud in the z -direction. [8] For future reference for the parameters appropriate to ^{23}Na , $N_o^{(3)} = 1.7 \times 10^4 / \Lambda$ if $\epsilon = (\lambda_o/R)^2 = 0.1$ for a trap with trap frequency 100 Hz in the radial direction. Here Λ is the anisotropy parameter R/R_z .
 - [10] *c.f.* for a scalar order parameter at this ϵ , a singly quantized vortex is energetically favorable for $0.45 < \tilde{\Omega} < 0.6$.

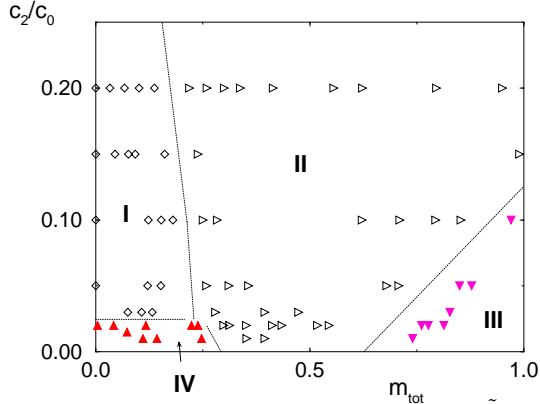


FIG. 1. The phase diagram for $\epsilon = 0.1$, $\tilde{\Omega} = 0.45$. I (diamonds): vortices in both u and d , configuration as in Fig 3 except for a possible adjustment of relative magnitudes of $|\Psi_{u,d}|$; II (triangles right): vortex in u with d core as in Fig 4; III (triangles down): vortex in u with mainly 0 core as in Fig 5; IV (triangles up): configuration as in Fig. 7. Dotted lines are guides to the eye.

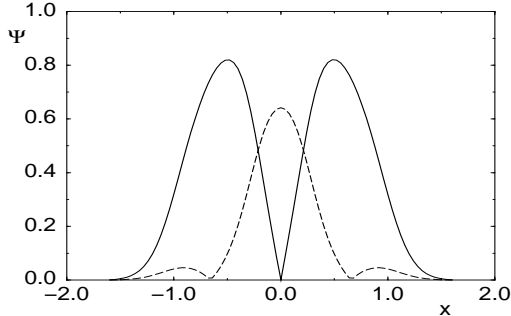


FIG. 2. CV for $\tilde{c}_2 = 0.2$, $\tilde{\Omega} = 0.45$. $m_{\text{tot}} = 0$. $|\Psi_0|$, full line; $|\Psi_u| = |\Psi_d|$, dashed.

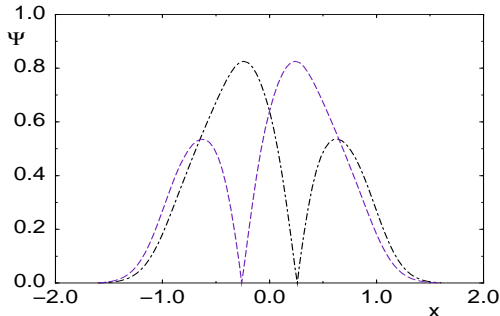


FIG. 3. The same CV as Fig 2, but with different quantization axis. $|\Psi_u|$, dashed-dotted; $|\Psi_d|$, dashed.

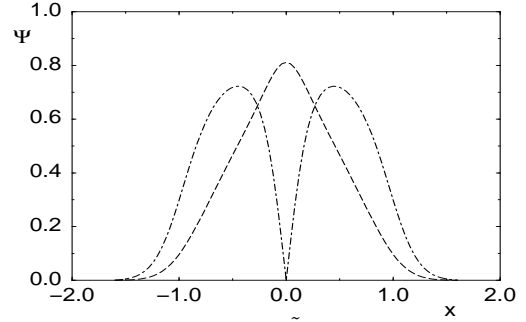


FIG. 4. CV for $\tilde{c}_2 = 0.2$, $\tilde{\Omega} = 0.45$, and $m_{\text{tot}} = 0.414$. $|\Psi_u|$, dashed-dotted; $|\Psi_d|$, dashed.

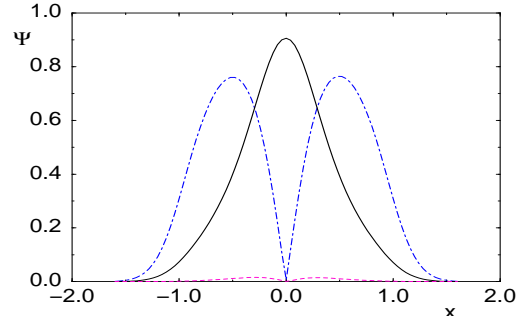


FIG. 5. CV for $\tilde{c}_2 = 0.02$, $\tilde{\Omega} = 0.45$, and $m_{\text{tot}} = 0.77$. $|\Psi_u|$, dashed-dotted; $|\Psi_0|$, full-line.

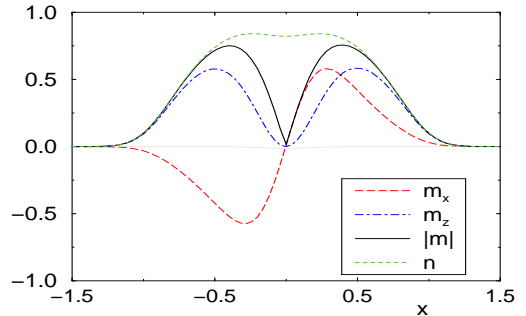


FIG. 6. Local magnetization for the CV of Fig 5.

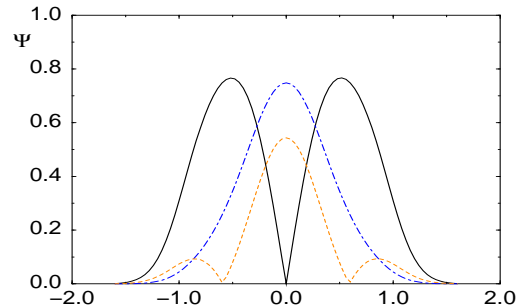


FIG. 7. CV for $\tilde{c}_2 = 0.02$, $\tilde{\Omega} = 0.45$, and $m_{\text{tot}} = 0.03$ ($H = 0$). $|\Psi_u|$, dashed-dotted; $|\Psi_0|$, full line; $|\Psi_d|$, dashed.

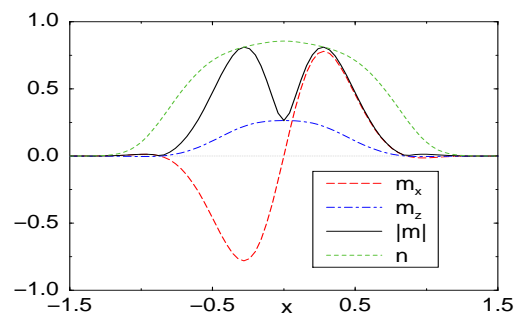


FIG. 8. Local magnetization and density for the CV of Fig 7.